J. Fluid Mech. (1991), *vol.* 232, *pp.* 357–375
Printed in Great Britain

The linear inviscid secondary instability of longitudinal vortex structures in boundary layers

By PHILIP HALL[1] AND NICOLA J. HORSEMAN[2]

[1] Department of Mathematics, University of Manchester, Oxford Road, Manchester M13 9PL, UK

[2] Mathematics Department, Exeter University, North Park Road, Exeter EX4 4QE, UK

(Received 8 October 1990)

The inviscid instability of a longitudinal vortex structure within a steady boundary layer is investigated. The instability has wavelength comparable with the boundary-layer thickness so that a quasi-parallel approach to the instability problem can be justified. The generalization of the Rayleigh equation to such a flow is obtained and solved for the case when the vortex structure is induced by curvature. Two distinct modes of instability are found; these modes correspond with experimental observations on the breakdown process for Görtler vortices.

1. Introduction

Our concern is with the unsteady three-dimensional breakdown of longitudinal vortices in incompressible boundary layers. Though we shall concentrate on the situation where the vortices are induced by streamline curvature, our analysis is equally relevant to secondary instability of the vortex structures produced in the later stages of boundary-layer transition as described recently by Hall & Smith (1991). It is well known that both steady and unsteady boundary layers are susceptible to the so-called Görtler vortex instability mechanism; this mechanism is identical to the Taylor vortex instability investigated by Taylor (1923). The latter instability is usually associated with the flow between rotating concentric cylinders but the terminology is equally relevant to, for example, the centrifugal instability of pressure-gradient flows in channels, Dean (1928), or that of a Stokes layer on a torsionally or laterally oscillating cylinder, Seminara & Hall (1975), Honji (1981), Hall (1984). The main distinguishing feature of the Görtler vortex is that it is a mechanism which is operational in a spatially varying flow. It is known from the recent work of Denier, Hall & Seddougui (1991) that non-parallel effects are particularly important at small vortex wavelengths.

We shall now discuss briefly some relevant experimental and theoretical results concerning the growth and breakdown of Görtler vortices in curved boundary layers; a more detailed account of that work can be found in Hall (1990). Perhaps the first experimental evidence for the existence of the instability mechanism predicted by Görtler (1940) is due to Lieppmann (1943, 1945), but the first detailed experimental investigation of the instability was described by Bippes (1972). More recently, significant contributions have been made by Aihara & Kohama (1981), and Swearingen & Blackwelder (1987). In the early stages of the vortices' development the disturbance field is steady and takes the form of spanwise-periodic counter-rotating vortices. Significantly these initial stages appear extremely sensitive to the upstream flow and often the initial periodicity of the flow is fixed by some type of

forcing mechanism at the wall. However, it is known from the work of Hall (1990) and Denier *et al.* (1991) that free-stream disturbances and wall roughness are both possible causes of the initial vortex growth. After the initial onset of the instability flow visualization and hot-wire measurements show that a finite-amplitude state, evolving in the flow direction, is generated as the boundary layer grows. At some stage further downstream this steady state undergoes a secondary instability to a three-dimensional time-dependent disturbance. Sometimes this instability leads to an unsteady wavy vortex flow of the type which causes the unsteady breakdown of Taylor vortices in the circumferential flow between cylinders of almost the same radius. In other situations the breakdown leaves the vortex boundaries flat but causes the generation of horseshoe vortices typical of the later stages of flat-plate boundary-layer transition. Thus it would appear that there are at least two distinct modes of instability of longitudinal vortex structures. In fact Tollmien–Schlichting waves can also be involved in the breakdown process if the wall curvature in the experimental facility is sufficiently small to postpone the onset of Görtler vortices to high enough Reynolds numbers where Tollmien–Schlichting waves are unstable.

A theoretical description of the onset of a wavy vortex structure in Görtler vortex flows has been given by Hall & Seddougui (1989). That calculation is appropriate to small-wavelength vortices where non-parallel effects are not important but nevertheless the results found by Hall & Seddougui were consistent with the experimental observations of Peerhossaini & Wesfreid (1988*a*, *b*). In particular Hall & Seddougui showed that two wavy vortex modes are possible in small-wavelength Görtler vortices; in particular these modes are localized in the normal direction in thin shear layers above and below the region of vortex activity as described by Hall & Lakin (1988). For vortex wavelengths comparable with the boundary-layer thickness the linear and nonlinear stages of vortex growth are described by non-parallel effects (Hall 1983, 1988), thus the mode identified by Hall & Seddougui is not easily investigated in this regime because it leads to a three-dimensional, unsteady Navier–Stokes calculation. However it would be extremely surprising if the wavy mode instability based on a three-dimensional unsteady Görtler vortex was not in operation at $O(1)$ vortex wavelengths. In this paper we shall concentrate on the question of whether some of the experimentally observed breakdown routes of Görtler vortices owe their origin to an inviscid instability mechanism. Interestingly, in their convincing theoretical description of the onset of wavy Taylor vortex flows Davey, DiPrima & Stuart (1968) suggested that the wavy vortex mode might well be of inviscid origin. Indeed, recent work by Bassom & Seddougui (1990), who investigated more fully the wavy vortex spectrum found by Hall & Seddougui, shows that some of the wavy modes are certainly of inviscid character. From the theoretical point of view the fact that $O(1)$-wavelength vortices evolve in a non-parallel manner means that the concept of a unique curve or growth rate is not tenable in the Görtler problem (Hall 1983, 1988). It is this property which distinguishes Görtler vortices from Tollmien–Schlichting waves, which occur at such high Reynolds numbers that they are adequately described by a quasi-parallel theory. This is also the main difference between Görtler and Taylor vortices; thus in a Taylor vortex experiment the control parameter governing the flow is constant in the steady regime, in the Görtler problem the downstream variable in effect plays the role of the control parameter. In the Taylor problem it is well-known that significant changes in flow properties occur when the control parameter is slightly increased; in the Görtler problem the experimentalist or theoretician is not able to restrict his attention to small increases in this parameter. For that reason it is not surprising that careful

experiments on Görtler vortices are not as common as those on the Taylor mechanism.

In this paper we shall in the first instance use the nonlinear scheme of Hall (1988) to determine the evolution of finite-amplitude $O(1)$-wavelength vortices in a curved boundary layer. We shall then investigate the instability of the new three-dimensional state at a given downstream position to an inviscid Rayleigh instability. These modes have spanwise and streamwise lengthscales comparable with the boundary-layer thickness so the stability problem formulated is a local one. The formulation of the problem and some particular solutions are given in §2. In §3 we describe a scheme used to solve the two-dimensional generalization of Rayleigh's equation found in §2. Finally in §4 we discuss our results and compare with experimental observations.

2. Formulation of the problem

Consider the flow of a viscous fluid of kinematic viscosity ν over a wall of variable curvature $a^{-1}K(x/l)$. Here a is a typical radius of curvature of the wall whilst l is a lengthscale in the flow direction. If U_0 is a typical value of the fluid speed at infinity then we define a Reynolds number Re by

$$Re = U_0 l/\nu, \tag{2.1}$$

and throughout this paper we shall consider the limit $Re \to \infty$ with the Görtler number G defined by

$$G = 2l/a\,Re^{\frac{1}{2}}, \tag{2.2}$$

held fixed. Of course it is possible to allow $l/a \to 0$, and $Re \to \infty$ such that $G \to 0$ or $G \to \infty$ but we isolate the above limit because it is known that instability occurs first for $G = O(1)$. In the absence of any longitudinal vortex structure in the flow we have a two-dimensional steady boundary-layer flow $U_0(\bar{u}(X,Y), \bar{v}(X,Y)Re^{-\frac{1}{2}}, 0)$ obtained by solving

$$\left.\begin{aligned} &\bar{u}_X + \bar{v}_Y = 0, \\ &\bar{u}\bar{u}_X + \bar{v}\bar{u}_Y = -\bar{p}_X + \bar{u}_{YY}, \\ &\bar{u} = \bar{v} = 0, \quad Y = 0, \\ &\bar{u} \to u_E(X), \quad y \to \infty. \end{aligned}\right\} \tag{2.3}$$

Here $(X, Y) = (x/l, Re^{\frac{1}{2}}, y/l)$, $\bar{p}$ is the streamwise pressure gradient associated with the flow, and $u_E(X)$ is the dimensionless free-stream speed. Now we suppose that the curvature of the wall induces a Görtler vortex velocity field defined by

$$\begin{aligned} \boldsymbol{u}/U_0 = \boldsymbol{u}_B(X,Y,Z) &= (\bar{u}, \bar{v}Re^{-\frac{1}{2}}, 0)\,(1 + O(Re^{-\frac{1}{2}})) \\ &+ (U(X,Y,Z), V(X,Y,Z)Re^{-\frac{1}{2}}, W(X,Y,Z)Re^{-\frac{1}{2}})\,(1 + O(Re^{-\frac{1}{2}})). \end{aligned} \tag{2.4}$$

Here Z is a dimensionless spanwise variable scaled on $Re^{-\frac{1}{2}}l$ and we assume that the flow is periodic in the spanwise direction with wavelength $\lambda = 2\pi/k$. If $P(X,Y,Z)$ is the dimensionless pressure field associated with (U, V, W) then, from Hall (1988), we see that the system of equations to determine the vortex field and induced mean flow is

$$U_X + V_Y + W_Z = 0, \tag{2.5a}$$

$$U_{YY} + U_{ZZ} - V\bar{u}_Y = \bar{u}U_X + U\bar{u}_X + \bar{v}U_Y + Q_1, \tag{2.5b}$$

$$V_{YY} + V_{ZZ} - GK\bar{U}U - P_Y = \bar{u}V_X + U\bar{v}_X + \bar{v}V_Y + V\bar{v}_Y + Q_2, \tag{2.5c}$$

$$W_{YY} + W_{ZZ} - P_Z = \bar{u}W_X + \bar{v}W_Y + Q_3, \tag{2.5d}$$

where

$$Q_1 = UU_X + VU_Y + WU_Z, \tag{2.6a}$$

$$Q_2 = UV_X + VV_Y + WV_Z + \tfrac{1}{2}GKU^2, \tag{2.6b}$$

$$Q_3 = UW_X + VW_Y + WW_Z. \tag{2.6c}$$

The above equations are to be solved subject to

$$U = V = W = 0, \quad Y = 0, \tag{2.7a}$$

$$U \to 0, \quad V \to \hat{V}(X), \quad W \to 0, \quad Y \to \infty, \tag{2.7b}$$

where $\hat{V}(X)$ is a function of X to be determined. The most notable feature of the above system is that P_X does not appear in the streamwise momentum equation so that the vortex equations are parabolic in X. The nonlinear Görtler vortex equations (2.5) were solved by Hall (1988) and the reader is referred to that paper for a discussion of an appropriate numerical scheme for their solution. We shall discuss the results of such a nonlinear calculation in the next section. Now let us turn to the possible instability of a nonlinear vortex flow to an inviscid travelling wave disturbance.

It is well known that inviscid disturbances vary in the streamwise direction on the lengthscale $Re^{-\frac{1}{2}}l$ so that their wavelength is comparable with the boundary-layer thickness. In addition the timescale for an inviscid disturbance is $lU_0^{-1}Re^{-\frac{1}{2}}$ so that we perturb the basic state by writing

$$\boldsymbol{u}/\boldsymbol{U}_0 = \boldsymbol{u}_B + \Delta(u(X,Y,X), v(X,Y,Z), w(W,Y,Z)) \exp\{\mathrm{i}Re^{\frac{1}{2}}\theta(X,T)\}, \tag{2.8}$$

where $T = tU_0/l$ and Δ is taken to be sufficiently small for linearization to be a valid procedure. Finally we take the corresponding pressure perturbation to be $\Delta P(X,Y,Z)\rho U_0^2 \exp\{\mathrm{i}Re^{\frac{1}{2}}\theta(X,T)$ where ρ is the fluid density. If we now write $\alpha = \theta_X$, $\alpha c = -\theta_T$ then we find that, in the limit $Re \to \infty$, the zeroth-order disturbance equations at the local position X are

$$\left.\begin{aligned} \mathrm{i}\alpha U + V_Y + W_Z &= 0, \\ \mathrm{i}\alpha\{\bar{U} - c\}U + V\bar{U}_Y &= -\mathrm{i}\alpha P, \\ \mathrm{i}\alpha\{\bar{U} - c\}V &= -P_Y, \\ \mathrm{i}\alpha\{\bar{U} - c\}W + W\bar{U}_Z &= -P_Z, \end{aligned}\right\} \tag{2.9}$$

where $\bar{U} = \bar{u} + U$ is the total downstream velocity field associated with the basic state in the presence of a longitudinal vortex field. Since viscous effects are negligible away from the wall (and any position where $\bar{U} = c$) the appropriate boundary conditions for (2.9) are

$$V = 0, \quad Y = 0, \infty. \tag{2.10}$$

Since the basic state about which we are performing an inviscid instability analysis is non-parallel it is not clear whether we should seek temporally or spatially growing modes. Here we shall concentrate on the temporal case and therefore seek eigenvalues of (2.9)–(2.10) with α real and c complex. Our primary aim is to find the fastest growing modes so we shall not seek eigenvalues appropriate to the neutral case with α and c real. A discussion of the critical layer structure of (2.9) when α and c are real can be found in Horseman (1991); essentially it is unchanged from that of the simpler situation when $\bar{U}$ is a function of Y alone. In general (2.9)–(2.10) must be solved

numerically; with this fact in mind it is convenient to eliminate U, V, W to give the pressure equation

$$\left\{\frac{\partial^2}{\partial Y^2}+\frac{\partial^2}{\partial Z^2}-\alpha^2\right\}P-\frac{2\bar{U}_Y P_Y}{\bar{U}-c}-\frac{2\bar{U}_Z P_Z}{\bar{U}-c}=0. \tag{2.11}$$

This equation must be solved subject to the conditions

$$P_Y=0, \quad Y=0, \quad P\to 0, \quad Y\to\infty, \tag{2.12}$$

and P must, of course, be periodic in Z. For a Görtler vortex flow $\bar{U}$ may be written as

$$\bar{U}=\bar{U}_0(X,Y)+\sum_1^\infty \bar{U}_n(X,Y)\cos nkZ, \tag{2.13}$$

so that (2.11) has solutions of the form

$$P=\sum_1^\infty P_n(X,Y)\sin nkZ, \tag{2.14a}$$

and

$$P=\hat{P}_0(X,Y)+\sum_1^\infty \hat{P}_n(X,Y)\cos nkZ. \tag{2.14b}$$

We refer to the above modes as 'odd' and 'even' respectively and we note that the odd mode leads to the 'wavy' vortex boundaries observed experimentally. In contrast the even mode corresponds to a time-dependent state in which the vortex boundaries remain flat, we conjecture that this mode leads to horseshoe vortices. As mentioned in the introduction there is experimental evidence for both of these modes. We also note that (2.14) can be generalized to allow for a more complicated spanwise dependence using Floquet theory. Such an approach would allow for the possibility of subharmonic modes, but since there is no experimental evidence for the importance of these modes, we do not investigate that possibility here.

The detailed calculations which we made were for the situation when $u_E = 1$ so that in the absence of a vortex field all inviscid disturbances are stable. However, other basic states are of practical relevance and we note that pressure-gradient-driven boundary layers can be inviscidly unstable in the absence of a vortex field. There is in fact one situation where some analytical progress can be made with (2.11)–(2.12); we refer to the case when the spanwise wavenumber k of the vortex is small. In this situation it is reasonable to expect that the inviscid disturbance behaves in a quasi-parallel manner in the spanwise direction. In that case we can drop the dependence of P with respect to Z and then P satisfies the ordinary differential equation

$$P_{YY}-\alpha^2 p-\frac{2\bar{U}_Y}{\bar{U}-c}P=0. \tag{2.15}$$

This is the Rayleigh pressure equation appropriate to a uni-directional flow with $\bar{U}$ a function of Y alone and we can think of the wave speed c as a function of the slow spanwise variable $\phi = kZ$. Intuitively we expect that the disturbance will concentrate itself where it is most unstable; thus for a given value of α suppose that $c = c^*$, $\partial c_i^*/\partial Z = 0$, $\partial^2 c_i^*/\partial Z^2 < 0$ at a point $Z = Z^*$. In fact for $\bar{U}$ appropriate to a Görtler vortex, see (2.13) above, it is easy to show that $kZ^* = (2n+1)\pi$ for $n = 1, 2, 3, \ldots$. Moreover, these positions correspond to the cell boundaries where upwelling occurs.

In order for us to determine the precise structure of the inviscid disturbance near $Z = Z^*$ it is necessary to define

$$\Phi = k^{\frac{1}{2}}[Z - Z^*], \tag{2.16}$$

and expand P in the form

$$P = P_0(\Phi, Y) + kP(\Phi, Y) + \dots . \tag{2.17}$$

In the neighbourhood of Z^*, $\bar{U}$ expands as

$$\bar{U} = U_0^*(Y) + k^2[Z - Z^*]^2 U_1^*(Y) + \dots, \tag{2.18}$$

where we note that the $O(k)$ term in this expansion is absent because c_i^* has a local maximum at $Z = Z^*$. Finally we expand the eigenvalue c in the form

$$c = c_0 + kc_1 + \dots . \tag{2.19}$$

If the above expansions are substituted into (2.11)–(2.12) and terms of order k^0, k are equated we obtain

$$\left.\begin{aligned} &\frac{\partial^2 P_0}{\partial Y^2} - \alpha^2 P_0 - \frac{2U_{0Y}^*}{U_0^* - c_0}\frac{\partial P_0}{\partial Y} = 0, \\ &P_{0Y} = 0, \quad Y = 0, \quad P_0 = 0, \quad Y \to \infty. \end{aligned}\right\} \tag{2.20a}$$

$$\frac{\partial^2 P_1}{\partial Y^2} - \alpha^2 P_1 - \frac{2U_{0Y}^*}{U_0^* - c_0}\frac{\partial P_1}{\partial Y} = \frac{2U_{0Y}^*}{U_0 - c_0}\Phi^2\left[\frac{U_{1Y}^*}{U_{0Y}^*} - \frac{U_1^*}{U_0^* - c_0}\right]P_{0Y} - \frac{\partial^2 P_0}{\partial \Phi^2} + \frac{2U_{0Y}^*}{(U_0^* - c_0^*)^2}c_1 P_{0Y}. \tag{2.20b}$$

The system (2.20a) is of course the local Rayleigh problem to determine the eigenvalue $c_0 = c_0(\alpha)$ whilst (2.20b) is an inhomogeneous version of (2.20a) and therefore only has a solution if a solvability condition is satisfied. We assume that (2.20a) has a solution and that it can be written in the form

$$P_0 = A(\Phi)\hat{P}_0(Y), \tag{2.21}$$

and the solvability condition on (2.20b) yields

$$A'' + \lambda_0 c_1 A - \lambda_1 \Phi^2 A = 0. \tag{2.22}$$

Here the constants λ_0 and λ_1 are given by

$$\lambda_1 = 2\int_0^\infty \frac{U_{0Y}^*}{U_0^* - c_0}\left[\frac{U_{1Y}^*}{U_{0Y}^*} - \frac{U_1^*}{U_0^* - c_0}\right]\hat{P}_0'(Y)\,\hat{Q}_0(Y)\,\mathrm{d}Y \Big/ \left(\int_0^\infty \hat{P}_0'(Y)\,\hat{Q}_0(Y)\,\mathrm{d}Y\right) \tag{2.23a}$$

$$\lambda_0 = -2\int_0^\infty \frac{U_{0Y}^*}{(U_0^* - c_0^*)^2}\hat{P}_0'\,\hat{Q}_0(Y)\,\mathrm{d}Y \Big/ \left(\int_0^\infty \hat{P}_0'(Y)\,\hat{Q}_0(Y)\,\mathrm{d}Y\right), \tag{2.23b}$$

where $\hat{Q}_0$ is the function adjoint to the eigensolution $\hat{P}_0(Y)$. The solutions of the linear amplitude equation (2.22) which decay when $|\Phi| \to \infty$ are

$$A = A_n(Y) = U(-n - \tfrac{1}{2}, \lambda_1^{\frac{1}{4}} 2^{\frac{1}{2}}\Phi), \quad n = 0, 1, 2, \tag{2.24}$$

where $U(-n-\frac{1}{2}, \lambda_1^{\frac{1}{4}}2^{\frac{1}{2}}\Phi)$ is a parabolic cylinder function; the complex correction to the wave speed is then given by

$$\lambda_0 c_1 / 2\lambda_1^{\frac{1}{2}} = -n - \tfrac{1}{2}. \tag{2.25}$$

Thus we have an infinite sequence of unstable eigenvalues; since $Z = Z^*$ is the most unstable point we know that for any vortex flow λ_0 and λ_1 are such that $\lambda_1^{\frac{1}{2}}/\lambda_0$ has negative imaginary part so that the $n = 0$ mode is the most unstable.

Hence in the small vortex wavenumber limit we see that Rayleigh modes occur at the spanwise locations where the flow is most unstable in a quasi-parallel sense. Alternatively, the structure described above is relevant for $O(1)$ vortex wavenumbers when the streamwise wavenumber α is large. Furthermore we note that in the situation described above the instability is associated with the inflexional nature of the velocity profile $\bar{U}$ in the Y-direction. Now we turn to the question of whether it is possible to determine an asymptotic structure associated with the inflexional nature of $\bar{U}$ in the Z-direction.

The basic downstream velocity component will have inflexion points with respect to the spanwise variable (i.e. where $\bar{U}_{ZZ} = 0$) at a given value of Y. However, these profiles will only lead to an inviscid instability if the latter mode can respond in a quasi-parallel manner to the inflexional profiles in the spanwise direction. In order for this to be the case the basic the flow must vary more quickly in the spanwise direction than in the normal one. Since the normal variation of the basic state is fixed by the boundary-layer thickness the only possibility then is to look at the situation when k is large. In that limit, based on the asymptotic structure of Hall (1982*a*, *b*), Hall & Lakin (1988) have given an asymptotic description of the vortex-driven mean state. Essentially the boundary layer is split into three regimes. In the main part of the boundary layer a finite-amplitude vortex drives a mean flow and $\bar{U}$ expands as

$$\bar{U} = \bar{U}_0(X, Y) + k^{-1}\bar{U}_1(X, Y)\cos kZ + \ldots. \tag{2.26}$$

We stress that $\bar{U}_0$ is driven by the vortex and has no relationship with the mean state which would exist in the absence of a vortex. The vortex function $\bar{U}_1$ is found to vanish at two positions Y_1 and Y_2 satisfying $0 < Y_1 < Y_2 < \infty$. Below Y_1 and above Y_2 the boundary-layer equations apply and there is no vortex flow. In fact the vortex activity is reduced to zero in the shear layers of thickness $k^{-\frac{2}{3}}$ centred on Y_1 and Y_2.

Suppose then that we seek a solution of (2.11)–(2.12) appropriate to the velocity field $\bar{U}$ given by (2.26) in the limit $k \to \infty$. At a given value of Y the function $\bar{U}$ has an inflexion point where $kZ = (n+\frac{1}{2})\pi$ for $n = 0, 1, \ldots$. Let us now seek a localized solution of (2.11)–(2.12) centred on some position $Y = \bar{Y}$ with $Y_1 < Y < Y_2$. Since the instability, if present, must be associated with the $O(k^{-1})$ term in (2.26) we require $\bar{U} - c = O(k^{-1})$. Thus we write

$$c = \bar{U}_0(\bar{Y}) + k^{-1}c_1 + \ldots, \tag{2.27a}$$

$$\alpha = \hat{\alpha}k + \ldots. \tag{2.27b}$$

The local eigenvalue problem at $\bar{Y}$ then reduces to

$$\frac{\partial^2 P}{\partial \tilde{Z}^2} - \hat{\alpha}^2 P + \frac{2\bar{U}_1(\bar{Y})\sin\tilde{Z}}{\bar{U}_1(\bar{Y})\cos\tilde{Z} - c_1}P_{\tilde{Z}} = 0, \quad \tilde{Z} = kZ, \tag{2.28}$$

which has solutions with c_1 complex. However, the vertical structure of p corresponds to a second-order turning point when described by a WKB expansion only if $\bar{U}_{0Y}(\bar{Y}) = 0$. In that situation the inviscid disturbance is trapped in a layer of depth $k^{-\frac{2}{4}}$ and the vertical structure is then expressible in terms of parabolic cylinder functions. However, Hall & Lakin found that for Görtler vortex flows $\bar{U}_0$ is a monotonically increasing function of Y in the region of vortex activity so the above type of localized mode cannot occur when a flow of the type (2.26) is driven by wall curvature; nevertheless we expect that this type of mode is physically relevant in other situations.

In the absence of a turning point for $\bar{U}_0$ a WKB description of the vertical

structure of the inviscid mode for $k \gg 1$ suggests that any localized mode should have its vertical structure described by Airy functions (Walton 1978; Soward & Jones 1983). For the flow given by (2.26) this suggests that the inviscid modes should be confined in a layer of depth k^{-1}. Interestingly enough this means that the inviscid mode has $\partial_Y \sim \partial_Z$ and the eigenfunction then satisfies a partial differential equation again. More precisely if we look for a mode trapped near $Y = \bar{Y}$ and write

$$\zeta = k\{Y - \bar{Y}\}, \quad \tilde{Z} = kZ,$$

then, if the expansions (2.27) are retained, the zeroth-order approximation to (2.12) becomes

$$\frac{\partial^2 P}{\partial \zeta^2} + \frac{\partial^2 P}{\partial \tilde{Z}^2} - \alpha^2 P - \frac{2\bar{U}_0'(\bar{Y}) P_\zeta}{\zeta \bar{U}_0'(\bar{Y}) + \bar{U}_1(\bar{Y}) \cos \tilde{Z} - c_1} + \frac{2\bar{U}_1(\bar{Y}) \sin \tilde{Z} P_{\tilde{Z}}}{\zeta \bar{U}_0'(\bar{Y}) + \bar{U}_1(\bar{Y}) \cos \tilde{Z} - c_1} = 0, \quad (2.29)$$

which must be solved subject to periodicity in $\tilde{Z}$ and $|P| \to 0$, $|\zeta| \to \infty$. As yet we have found no solutions of this eigenvalue problem but further investigations are being carried out. However it is interesting to note that (2.29) is applicable to the inviscid stability problem for a general velocity field consisting of a spanwise-periodic velocity field superimposed on a linear shear flow. Thus, if unstable solutions of (2.29) can be found, they are of relevance to a wide class of shear flows.

The only alternative localized structure for the inviscid mode in the large-wavenumber limit would be one which takes account of the localized structure of the mean state near $Y = Y_1, Y_2$. As mentioned above, the vortex activity of the mean state decays to zero in layers of depth $k^{-\frac{2}{3}}$ near Y_1, Y_2. In fact $\bar{U}$ in these layers expands as

$$\bar{U} = U_{00} + k^{-\frac{2}{3}}\{Y - Y_j\} U_{01} + k^{-\frac{4}{3}}\{U_{02}(k^{\frac{2}{3}}[Y - Y_j]) + U_{03}(k^{\frac{2}{3}}[Y - Y_j]) \cos \tilde{Z}\} + \ldots, \quad j = 1, 2.$$

The mean shear term proportional to U_{01} again prevents a localized inviscid mode structure based on parabolic cylinder functions. In fact, Hall & Seddougui (1989) show that the basic state in the shear layers at Y_1, Y_2 is susceptible to a (viscous) wavy vortex mode of instability. Thus we believe that, unless unstable solutions of (2.29) can be found, there are no vertically localized eigenfunctions associated with the highly inflexional velocity profiles in the spanwise direction.

3. A numerical scheme for the solution of the generalized Rayleigh pressure equation

A suitable scheme to integrate the nonlinear Görtler vortex equations (2.5) has been described by Hall (1988) so we assume that $\bar{U}$, the total downstream velocity component, is known and outline a scheme to solve (2.11). For computational purposes it is convenient to restrict Z in (2.11) to one half of a vortex wavelength and determine boundary conditions at $Z = 0, \pi/k$ appropriate to the odd and even modes (2.14*a*, *b*). From (2.14) it is easy to show that appropriate conditions for the odd and even modes are

Odd modes:
$$\left.\begin{aligned} &P_Y = 0, \quad Y = 0, \quad P \to 0, \quad Y \to \infty, \\ &P = 0, \quad Z = 0, \quad \pi/k; \end{aligned}\right\} \quad (3.1)$$

Even modes:
$$\left.\begin{aligned} &P_Y = 0, \quad Y = 0, \quad P \to 0, \quad Y \to \infty, \\ &P_Z = 0, \quad Z = 0, \quad \pi/k. \end{aligned}\right\} \quad (3.2)$$

For convenience we define the functions F, G by

$$F = \frac{-2\bar{U}_Y}{\bar{U}-c}, \quad G = \frac{-2\bar{U}_Z}{\bar{U}-c} \tag{3.3a, b}$$

and we define a grid in the Z, Y-directions by writing

$$Z_j = \frac{(j-1)}{(M-1)}\frac{\pi}{k} = (j-1)b, \quad j = 1, 2, \ldots, M,$$

$$Y_i = \frac{(i-1)}{(N-1)}Y_\infty = (i-1)h, \quad n = 1, 2, \ldots, N.$$

Thus b and h are the step lengths in the Z- and Y-directions respectively. Suppose then that P_{ji} denotes P evaluated at $(Z, Y) = (Z_j, Y_i)$. We now define the vector $\boldsymbol{\xi}$ by

$$\boldsymbol{\xi} = \begin{bmatrix} \boldsymbol{P}_1 \\ \boldsymbol{P}_2 \\ \vdots \\ \boldsymbol{P}_N \end{bmatrix}, \quad \text{where} \quad \boldsymbol{P}_j = \begin{bmatrix} P_{1j} \\ \vdots \\ P_{Mj} \end{bmatrix} \quad \text{for} \quad j = 1, N,$$

and if the derivatives in (2.11) are approximated using central differences it follows that the discretized form of (2.11) becomes

$$\begin{Bmatrix} \boldsymbol{B}_1 \boldsymbol{C}_1 & & \\ \boldsymbol{A}_2 \boldsymbol{B}_2 \boldsymbol{C}_2 & & 0 \\ 0 & \ldots & \ldots \\ 0 & \boldsymbol{A}_N \boldsymbol{B}_N & \end{Bmatrix} \boldsymbol{\xi} = 0. \tag{3.4}$$

Here $\boldsymbol{A}_i, \boldsymbol{C}_i$ are diagonal matrices defined by

$$\boldsymbol{A}_i = \begin{Bmatrix} \ddots & & \\ & \frac{1}{h^2} - \frac{F_{ji}}{2h} & \\ & & \ddots \end{Bmatrix}, \quad \boldsymbol{C}_i = \begin{Bmatrix} \ddots & & \\ & \frac{1}{h^2} + \frac{F_{ji}}{2h} & \\ & & \ddots \end{Bmatrix}, \tag{3.5a, b}$$

whilst $\boldsymbol{B}_i$ is defined by

$$\boldsymbol{B}_i = \begin{Bmatrix} -\frac{2}{h^2} - \frac{2}{b^2} - \alpha^2 & \frac{1}{b^2} + \frac{G_{ji}}{2b} & 0 & \ddots & \\ \ddots & & \ddots & & \\ \frac{1}{b^2} + \frac{G_{ji}}{2b} & & \left(-\frac{G_{ji}}{2b} + \frac{1}{b^2}\right) & \left(-\frac{2}{h^2} - \frac{2}{b^2} - \alpha^2\right) & \left(\frac{1}{b^2} + \frac{G_{ji}}{2b}\right) \\ & & \ddots & & \end{Bmatrix}. \tag{3.5c}$$

In order to take care of the boundary conditions at $Y = 0$ the matrix $\boldsymbol{C}_1$ is redefined by writing

$$\boldsymbol{C}_1 \to \boldsymbol{C}_1 + \boldsymbol{A}_1.$$

If the system of linear equations (3.4) has a non-trivial solution then we have an eigenvalue $c = c(\alpha)$ of (2.11)–(2.12). The system (3.4) is of block tri-diagonal form and

so we can make use of this structure to speed up the calculations. In fact we solved a modified form of (3.4) by first replacing the boundary condition at $Y = 0$ by

$$P_Y = 1, \quad Y = 0.$$

This leads to an inhomogeneous form of (3.4) which can be solved for ξ using a standard block tri-diagonal solver. Having solved this system we then iterate on c until

$$\left\{ \int_0^{\pi/k} P^2 \, \mathrm{d}Z \right\}^{-1} \Bigg|_{Y=0} \to 0.$$

In effect this enables us to satisfy the boundary condition $P_Y = 0$, $Y = 0$. Solutions of (3.4) obtained in this way were checked by back-substitution into that equation. Typically we found that it is necessary to use 600 points in the Y-direction and 60 in the spanwise direction in order to calculate growth rates correct to two significant figures. However, we shall be more precise about the parameter values used in the following section.

4. Results and discussion

Our primary aim is to see if we can explain theoretically the experimentally observed description of the unsteady breakdown of steady longitudinal vortices induced by wall curvature. In particular we will focus on the experiments of Swearingen & Blackwelder (1987) who have given a detailed quantitative description of the breakdown process. First we shall give results which indicate that the nonlinear vortex calculations of the type discussed by Hall (1988) do indeed capture the essential details of the steady evolution of vortices as measured by Swearingen & Blackwelder (1987).

The experiments of Swearingen & Blackwelder were performed in a wind tunnel with a concave section of radius of curvature 320 cm and a free-stream speed of 500 cm/s. We note that in this configuration Tollmien–Schlichting waves are stable in the regime where Görtler vortices develop. The vortices were visualized by smoke and velocity fields were measured by a hot wire. In figure 1 we compare our results for the displacement thickness and wall shear obtained using the numerical scheme of Hall (1988) with the experimental results of Swearingen & Blackwelder for the case of a vortex of wavelength 1.8 cm. The calculations were started at a distance of 10 cm along the wall and the vortex amplitude was estimated from the experimental observation. In order to compare with experimental observations we have computed the wall shear and the displacement thickness in the low- and high-speed regions. Note here that the low- and high-speed regions correspond respectively to where upwelling and downwelling occur. We see that the computations predict the same kind of trends as observed experimentally upto a distance of 100 cm from the leading edge. Beyond that position the calculations diverge from the observations and in fact at a distance of about 120 cm from the leading edge the computations predict reversed flow and are therefore no longer valid. However, we believe that the reason why the calculations and observations diverge beyond $x = 120$ cm is that by this stage the vortex state has suffered a bifurcation to a three-dimensional time-dependent state. Below we shall show results that suggest that this breakdown is due to the instability mechanisms discussed in §2. Before discussing our results for the breakdown problem we will point out some relevant details of experimental observations concerning breakdown.

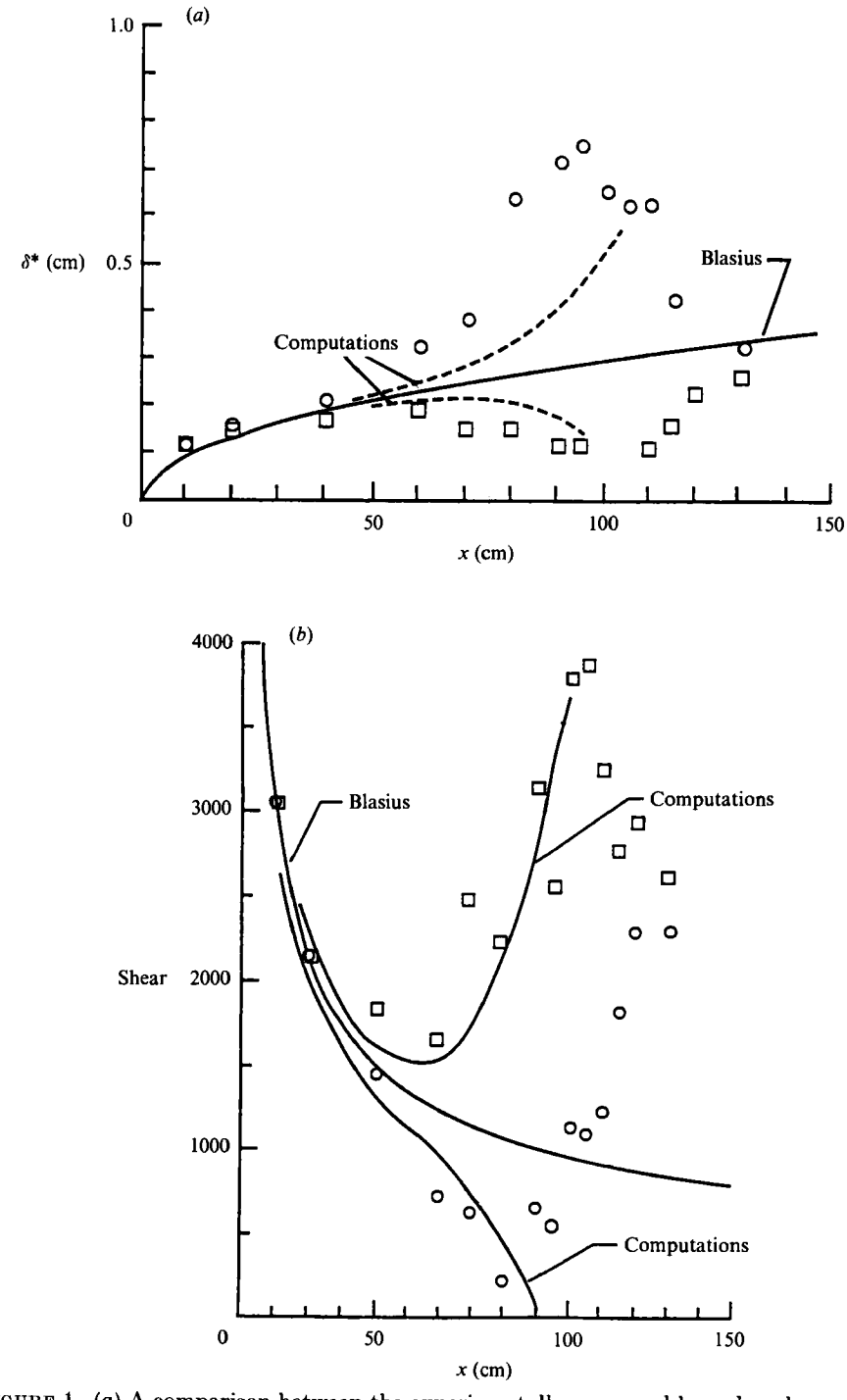

FIGURE 1. (*a*) A comparison between the experimentally measured boundary-layer thickness and that calculated using the method of Hall (1988). (*b*) A comparison between the wall shear measured experimentally and that predicted by the method of Hall (1988). ○, Low-speed region; □, high-speed region.

We refer first to figure 14 (*a*, *b*, *c*) of Swearingen & Blackwelder which shows smoke visualizations of the breakdown process for Görtler vortices. The visualizations correspond to an initial vortex state of wavelength 2.3 cm and show conclusively that there are at least two types of breakdown that can occur. First there is a sinuous or varicose mode in which the vortex boundaries become wavy in the manner typical of secondary instabilities of Taylor vortex flows. The second mechanism leaves the vortex boundaries flat and the smoke patterns indicate the presence of a horseshoe vortex typical of the later stages of transition in a flat-plate boundary layer. We shall show below that the theory of §2 can describe both types of process and that the horseshoe and vortex modes are to be associated with the even and odd modes of the inviscid stability equations. We further note that previous investigations, e.g. Bippes (1972), Aihara & Koyama (1981), have identified the two breakdown processes discussed above; we concentrate on the experiments of Swearingen & Blackwelder because the latter authors give the most detailed measurements in the breakdown regime. Finally, before discussing our results, we note that Swearingen & Blackwelder reported that the sinuous mode was the most preferred mechanism in their experiments. The downstream wavelength of this mode is estimated to be about 4.2 cm from their figure 14(*c*), and they give a value of about 130 Hz for the measured frequency of this mode.

In order to generate a basic state to be used as a basis for the theory of §2 we considered the configuration discussed above which we recall corresponds to a spanwise wavelength of about 2.3 cm. The linearized Görtler vortex equations were integrated for $x = 30$ to 60 cm using the initial condition

$$U = Y^6 \exp[-Y^2/2X], \quad V = 0$$

of Hall (1983). At $x = 60$ cm the nonlinear terms were switched on and the initial r.m.s. value of the vortex was estimated from figure 17 of Swearingen & Blackwelder. In figure 2 we show contours of constant $\bar{U}$ at $x = 70, 80, 90, 100$ cm. We see that this figure agrees qualitatively with figure 11 of Swearingen & Blackwelder. At $x = 100$ cm the calculated contours do not show the pronounced 'mushroom' structure shown in the experimental results but we note here that improved agreement with the experimental results can be found by 'tuning' the position where nonlinear effects are switched on. More precisely the increased vortex activity observed experimentally can be predicted if nonlinear effects are switched on well beyond $x = 60$ cm. However, we do not pursue this type of optimization procedure because it is, of course, not justified since there is certainly vortex activity at $x = 60$ cm.

Our calculations were almost exclusively for the basic state discussed above for $x = 100$ cm; this restriction was necessary because of the computational expense of the solution of (2.11)–(2.12). In order to calculate the eigenvalues of that system to the graphical accuracy of the figures which follow we used 600 points in the vertical direction with a step length $h = 0.25$ and 60 points in the spanwise direction (for a half-wavelength).

In the first instance we consider the odd modes of instability associated with (2.11)–(2.12). In figure 3(*a*) we show αc_i as a function of α for the two most unstable odd modes at $x = 100$ cm. We note that since eigenvalues of (2.11) occur in complex-conjugate pairs the eigenvalues shown do indeed correspond to unstable disturbances. Also shown is the only unstable mode we were able to locate at $x = 80$ cm. We see that the fastest growing mode at $x = 100$ cm occurs when $\alpha \sim 0.037$ and this corresponds to a downstream wavelength of about 3 cm. Since the odd mode leads

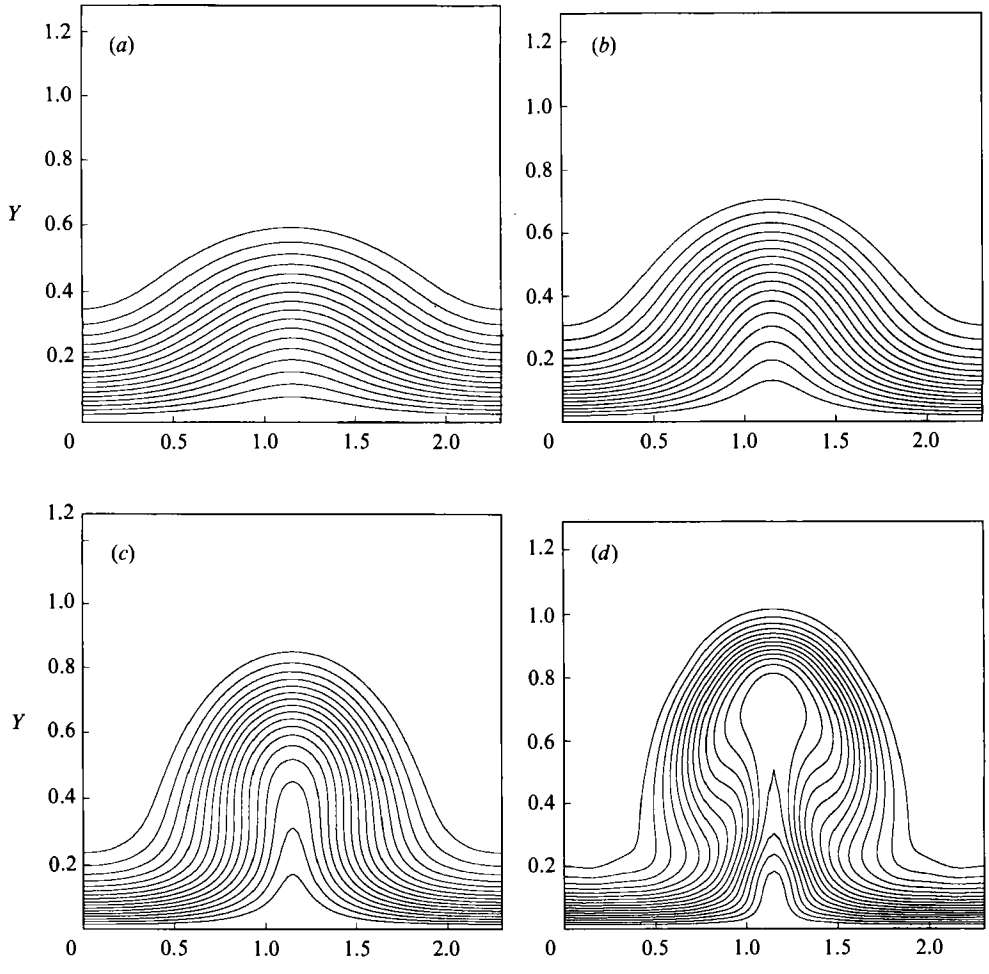

FIGURE 2. Contours of constant values of $\bar{U}$ at (*a*) $x = 70$ cm, (*b*) 80, (*c*) 90, (*d*) 100.

to wavy vortex boundaries this mode corresponds to the varicose mode of Swearingen & Blackwelder. Thus the predicted downstream wavelength of about 3 cm corresponds to an experimentally observed value of about 4.2 cm. Figure 3(*b*) shows the frequency of these modes as functions of α, the fastest growing mode with $\alpha = 0.037$ corresponds to a frequency of 110 Hz; again this compares favourably with the experimentally measured value of 130 Hz. Later we shall point out why it would be unreasonable, or fortuitous, to obtain better agreement with the experimental results. Now let us turn to the even solutions of the pressure disturbance equations.

In figure 4(*a*) we show the growth rate of the first two unstable even modes at $x = 100$ cm; we note that no unstable modes were found at $x = 80$ cm. The corresponding frequencies of these modes are shown in figure 4(*b*). A significant result is that at $x = 100$ cm the fastest growing odd mode has a growth rate twice as large as that of the fastest growing even mode. This is consistent with the observations of Swearingen & Blackwelder who found that the sinuous mode was the most easily excited mode during transition.

We now consider the flow fields associated with the fastest growing even and odd modes at $x = 100$ cm. The velocity eigenfunction associated with the solution was

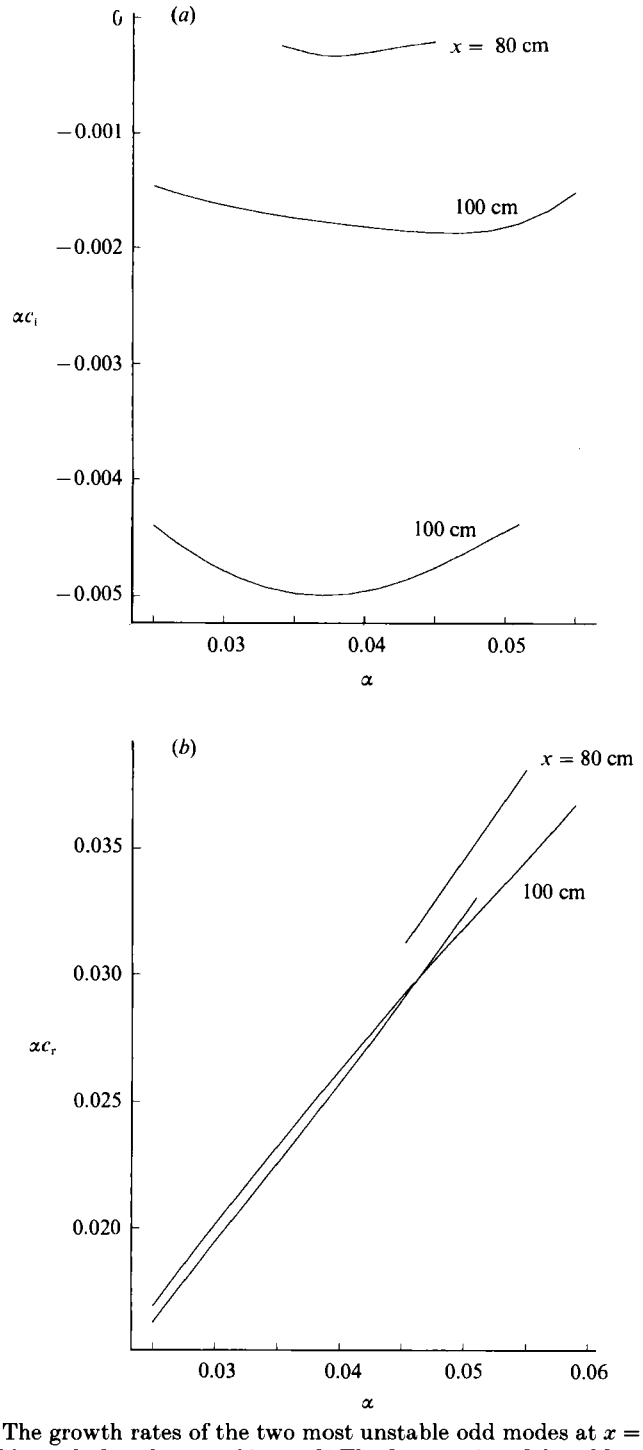

FIGURE 3. (*a*) The growth rates of the two most unstable odd modes at $x = 100$ cm. Also shown is the only unstable mode found at $x = 80$ cm. (*b*) The frequencies of the odd modes at $x = 80$, 100 cm.

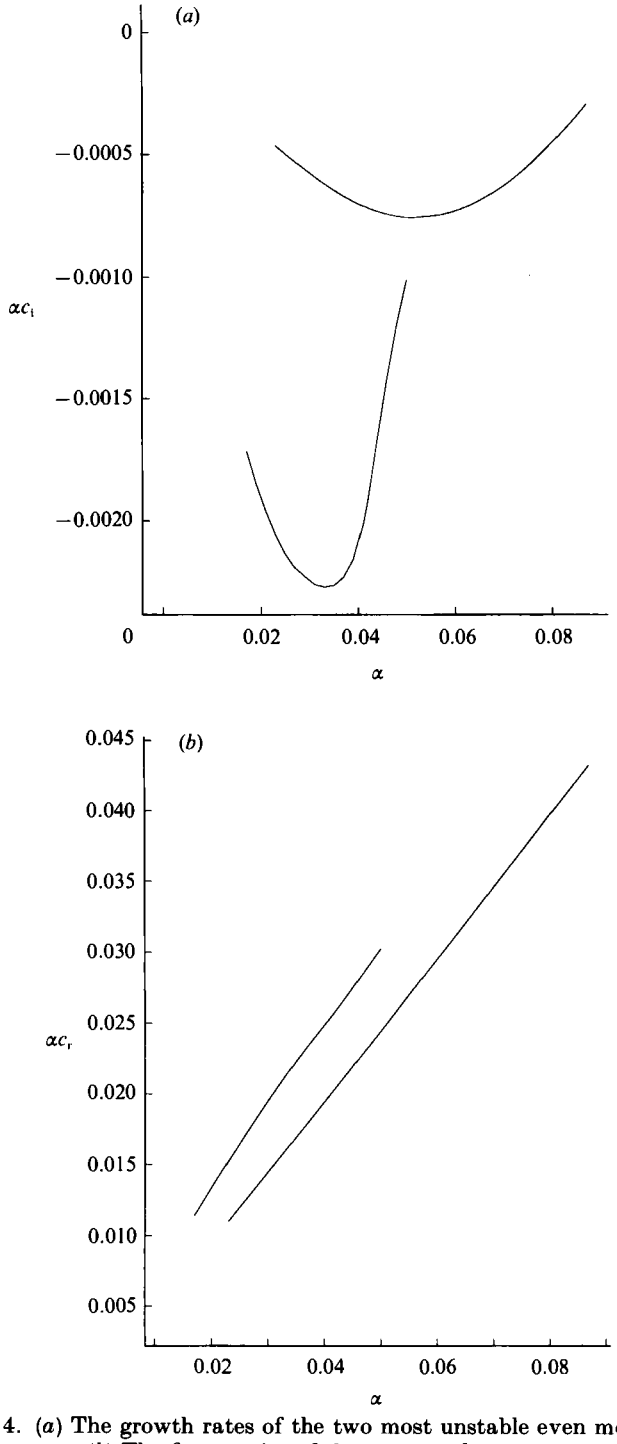

FIGURE 4. (*a*) The growth rates of the two most unstable even modes at $x = 100$ cm. (*b*) The frequencies of the even modes at $x = 100$ cm.

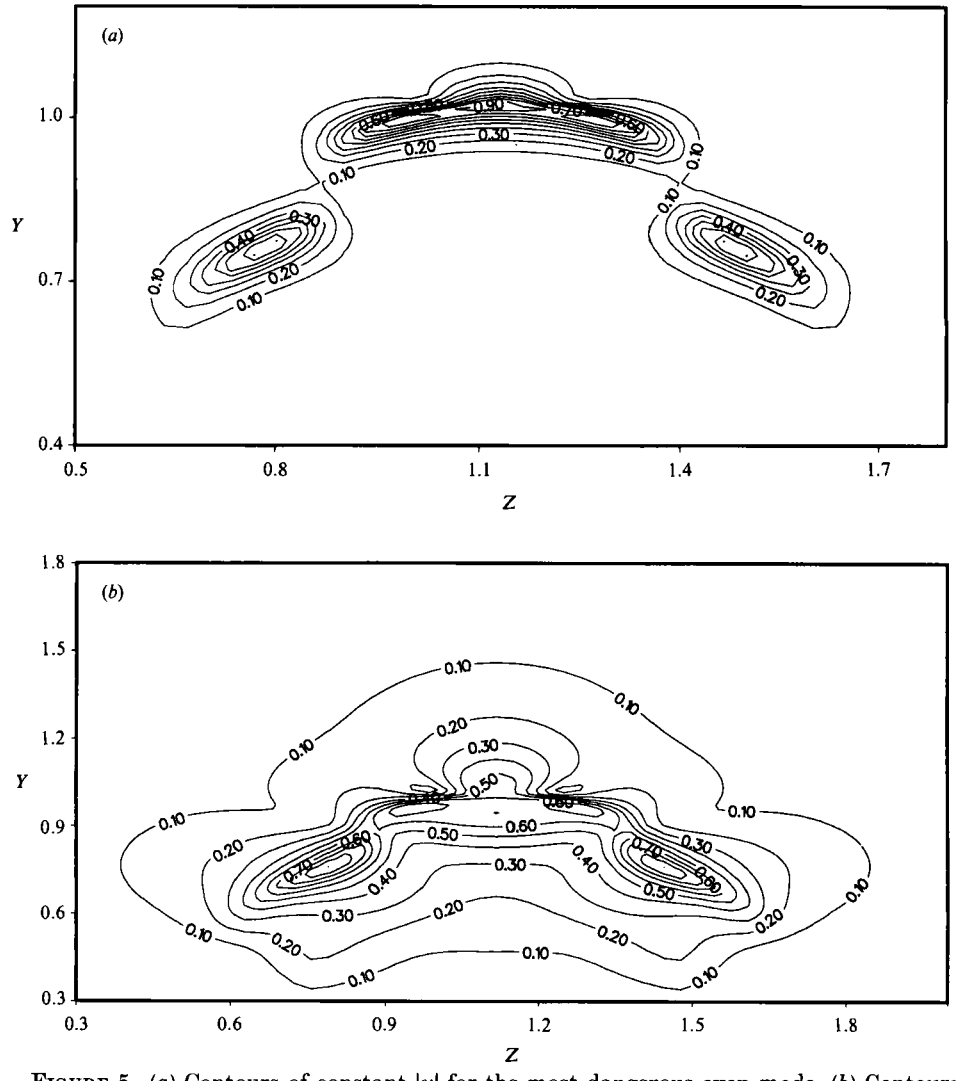

FIGURE 5. (*a*) Contours of constant $|u|$ for the most dangerous even mode. (*b*) Contours of constant $|v|$ for the most dangerous even mode.

normalized such that the maximum value of $|v|$ was unity in each case. Figure 5(*a*, *b*) shows contours of constant $|u|, |v|$ in the (Y, Z)-plane for the fastest growing even mode whilst figure 6(*a*, *b*) shows the corresponding functions for the fastest growing odd mode. We see that in each case the downstream velocity component is an order of magnitude larger than the Y-component. Again we see in each case that the downstream velocity field is much more concentrated than the normal one. Indeed the downstream velocity components are concentrated in the flow field in the region where $\bar{U} - c$ is small; in other words the inviscid mode localizes itself in a region which would develop into a critical layer in the neutral case. A major difference between the $|u|$ structure for the even and odd modes is that the even mode spans the position where upwelling occurs.

The velocity fields shown in figures 5(*b*) and 6(*b*) are to be compared with figure 16 of Swearingen & Blackwelder at $x = 100$ cm. We note that the experimental results show the flow field over two wavelengths and that the position $Z = 1.15$ in our

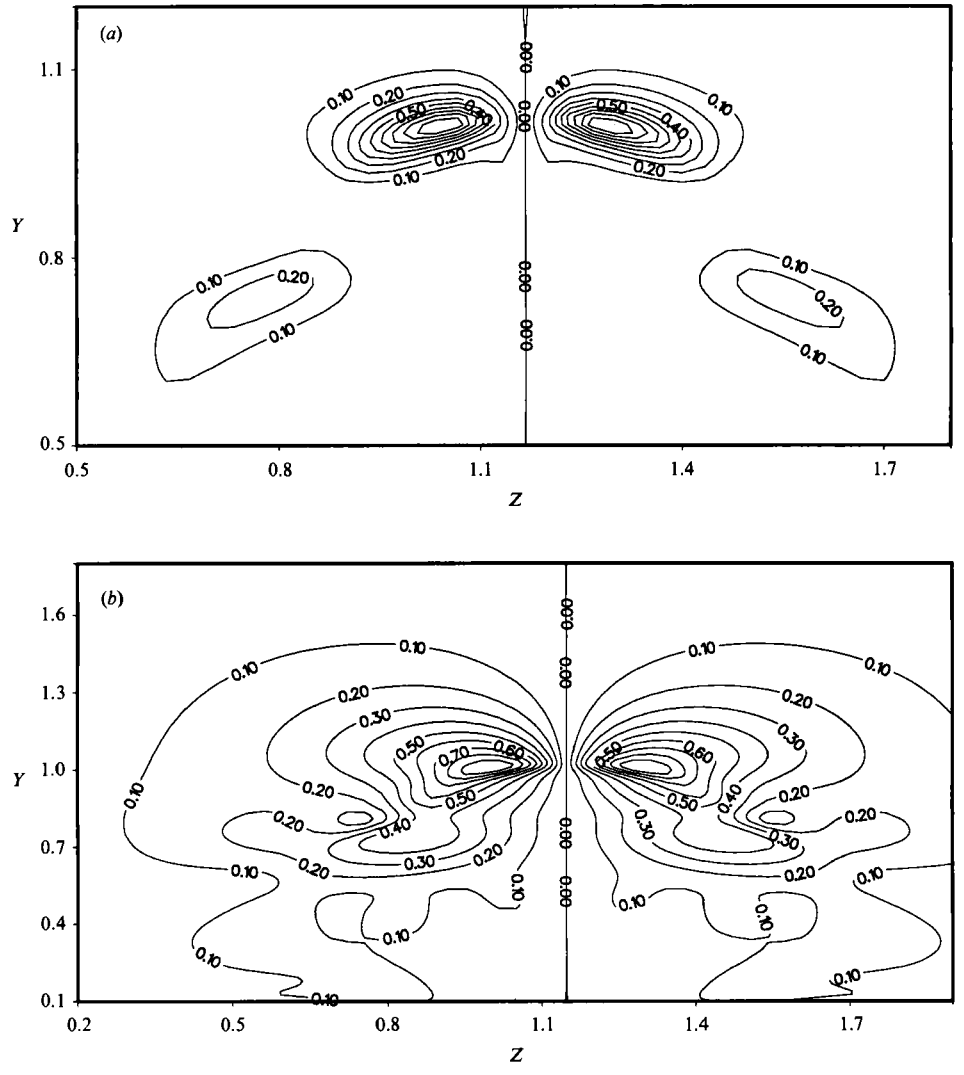

FIGURE 6. (*a*) Contours of constant $|u|$ for the most dangerous odd mode. (*b*) Contours of constant $|v|$ for the most dangerous odd mode.

work corresponds to the locations $z = 1.15, -1.15$ cm in the notation of Swearingen & Blackwelder. The calculations for both modes produce a velocity field concentrated in the region where the experiments produced the most significant disturbances. In fact the odd mode shown in figure 6(*b*) qualitatively resembles the experimental results away from the wall. Since the theory we have developed is inviscid we cannot hope to capture the experimentally observed disturbance structure close to the wall.

Our calculations suggest that each mode is unstable for a finite band of wavenumbers; probably the lower end of this range is at zero wavenumber. The numerical scheme we used fails if the wave speed is real, in which case there exists a critical layer in the flow, see Horseman (1991). Indeed if any of the growth rate curves are followed towards the horizontal axis (2.11) becomes progressively more expensive to solve since the equation is tending to become singular. For that reason we did not attempt to search for neutral modes by calculating unstable modes at

smaller and smaller growth rates; clearly any attempt to find the neutral modes must be based on a scheme which takes account of the disturbance structure at the critical layer. Since our main aim was to show that Görtler vortex flows are inviscidly unstable we choose not to tackle the neutral case, though the required structure at the critical layer is given in Horseman (1991).

Finally we close with a few words concerning the agreement of our results with the experimental observations. Essentially we wish to explain why it would be unreasonable to expect agreement better than that found above. The reason why we believe that this is the case is that the nonlinear Görtler vortex equations are parabolic in X. This means that the vortex flow at a given location depends on its upstream history so that the finite-amplitude vortex which we calculated as a basis for the stability calculations would be altered if the position where it was inserted into the flow was changed. We recall that the finite-amplitude state we calculated was introduced into the flow 60 cm from the leading edge. If this position is varied we find that the agreement between the calculations and experiments shown in figure 1 can be tuned to obtain optimum agreement. Typically we find that the flow properties shown in figure 1 vary by about 10% if the initial position of the vortex is pushed back as far as say 20 cm from the leading edge. Some limited calculations of the stability problem for flows calculated with these different initial vortex locations indicated a similar change in magnitude of the growth rates. Of course we could fix the initial vortex location so as to optimize the agreement between the basic state calculated numerically and that found experimentally. We choose not to do that because there is no justification for such a procedure; indeed it might be argued that the inherent non-uniqueness of the Görtler problem is present in the experiments as well. However, it can be said that the calculations we have carried out reproduce several key features of the experiments; to further optimize the agreement between theory and experiment would require an inordinate amount of computer time to reproduce features of an experiment which might itself not be precisely reproducible.

The authors wish to thank SERC and USAF for support for part of the work reported on above. Further thanks are due to ICASE where part of this work was carried out by one of us (P.H.). The authors also wish to thank the referees of this paper for their useful comments.

REFERENCES

AIHARA, Y. & KOHAMA, H. 1981 Secondary instability of Görtler vortices: Formation of periodic three-dimensional coherent structure. *Trans. Japan Soc. Aero. Sci.* **24**, 78.

BASSOM, A. P. & SEDDOUGUI, S. O. 1990 The onset of time-dependence and three-dimensionality in Görtler vortices: neutrally stable wavy modes. *J. Fluid Mech.* **220**, 661.

BIPPES, H. 1972 Experimental study of the laminar-turbulent transition of a concave wall in a parallel flow. *NASA TM* 75243.

DAVEY, A., DIPRIMA, R. C. & STUART, J. T. 1968 On the instability of Taylor vortices. *J. Fluid Mech.* **31**, 17.

DEAN, W. R. 1928 Fluid motion in a curved channel. *Proc. R. Soc. Lond.* A **121**, 402.

DENIER, J. P., HALL, P. & SEDDOUGUI, S. O. 1991 On the receptivity problem for Görtler vortices: vortex motions induced by wall roughness. *Phil. Trans. R. Soc. Lond.* A **335**, 51.

GÖRTLER, H. 1940 Uber eine dreidimensionale instabilität laminare Grenzschubten an Konkaven Wänden. *NACA TM* 1357.

HALL, P. 1982*a* Taylor–Görtler vortices in fully developed or boundary-layer flows. *J. Fluid Mech.* **124**, 475.

HALL, P. 1982*b* On the nonlinear evolution of Görtler vortices in non-parallel boundary layers. *J. Inst. Maths Applics* **29**, 173.

HALL, P. 1983 The linear development of Görtler vortices in growing boundary layers. *J. Fluid Mech.* **130**, 41.

HALL, P. 1984 On the stability of the unsteady boundary layer on a cylinder oscillating transversely in a viscous fluid. *J. Fluid Mech.* **146**, 347.

HALL, P. 1988 The nonlinear development of Görtler vortices in growing boundary layers. *J. Fluid Mech.* **193**, 247.

HALL, P. 1990 Görtler vortices in growing boundary layers: the leading edge receptivity problem, linear growth and the nonlinear breakdown stage. *Mathematica* **37**, 151.

HALL, P. & LAKIN, W. D. 1988 The fully nonlinear development of Görtler vortices in growing boundary layers. *Proc. R. Soc. Lond.* A **415**, 421.

HALL, P. & SEDDOUGUI, S. 1989 On the onset of three-dimensionality and time-dependence in Görtler vortices. *J. Fluid Mech.* **204**, 405.

HALL, P. & SMITH, F. T. 1991 On strongly nonlinear vortex/wave interactions in boundary-layer transition. *J. Fluid Mech.* **227**, 641.

HONJI, H. 1981 Streaked flow around an oscillating cylinder. *J. Fluid Mech.* **107**, 509.

HORSEMAN, N. J. 1991 Some centrifugal instabilities in viscous flows. Ph.D. thesis, Exeter University.

LIEPMANN, H. W. 1943 Investigations on laminar boundary layer stability and transition on curved boundaries. *NACA Wartime Rep.* W107.

LIEPMANN, H. W. 1945 Investigation of boundary layer transition on concave walls. *NACA Wartime Rep.* W87.

PEERHOSSAINI, H. & WESFREID, J. E. 1988*a* On the inner structure of streamwise Görtler rolls. *Intl J. Heat Fluid Flow* **9**, 12.

PEERHOSSAINI, H. & WESFREID, J. E. 1988*b* Experimental study of the Taylor–Görtler instability. In *Propagation in Systems Far from Equilibrium* (ed. J. E. Wesfreid, H. R. Brand, P. Manneville, G. Albinet & N. Boccara). Springer Series in Synergetics, vol. 41, pp. 399. Springer.

SEMINARA, G. & HALL, P. 1975 Centrifugal instability of a Stokes layer: linear theory. *Proc. R. Soc. Lond.* A **350**, 299.

SOWARD, A. M. & JONES, C. A. 1983 The linear stability of the flow in the narrow gap between concentric rotating spheres. *Q. J. Mech. Appl. Maths* **36**, 19.

SWEARINGEN, J. D. & BLACKWELDER, R. F. 1987 The growth and breakdown of streamwise vortices in the presence of a wall. *J. Fluid Mech.* **182**, 255.

TAYLOR, G. I. 1923 Stability of a viscous liquid contained between two rotating cylinders. *Phil. Trans. R. Soc.* A **223**, 289.

WALTON, I. C. 1978 The linear stability of the flow in a narrow spherical annulus. *J. Fluid Mech.* **86**, 673.